Chemical Engineering Journal 496 (2024) 154002

Contents lists available at ScienceDirect

Chemical Engineering Journal

journal homepage: www.elsevier.com/locate/cej

Phase separation behavior and CO_2 absorption kinetic analysis of DETA/DEA/DMAC biphasic absorbent

Zhipeng Chen [a], Tao Wang [a,*], Chao Li [a], Mengxiang Fang [a,*], Wei Chen [c], Ximing Hu [c], Yan Shao [d], Zhihao Liu [d], Wei Zhang [b], Li Zhang [b], Wenyang Fan [b], Shaojuan Zeng [e]

[a] State Key Laboratory of Clean Energy Utilizasstion, Zhejiang University, Hangzhou, China
[b] Zhejiang Tiandi Environmental Protection Technology Co. Ltd., Hangzhou, China
[c] Qingshanhu Energy Research Center, Zhejiang University, Hangzhou, China
[d] China City Environment Protection Engineering Limited Company,Wuhan,China
[e] Institute of Process Engineering, Chinese Academy of Sciences, Beijing 100190, China

ARTICLE INFO

Keywords:
Biphasic absorbent
Phase separation
Absorption mass transfer
Kinetic mechanism
Wetted wall column

ABSTRACT

Lower regeneration energy and superior cyclic capacity have enabled biphasic absorbents great potential in the area of flue gas CO_2 capture. The liquid film mass transfer coefficient(k_L) is a vital parameter in the development of absorbents with efficient CO_2 absorption mass transfer performance, while the phase separation behavior of biphasic solutions could be an essential factor for the absorption mass transfer and the stability of absorber. However, systemic kinetic research towards biphasic absorbents, especially the impact of phase separation behavior, is limited. In this study, a typical amide-based biphasic absorbent diethylenetriamine(DETA)/diethanolamine(DEA)/N, N-dimethylacetamide(DMAC) which has achieved great reduction in regeneration energy, was selected as the subject of kinetic investigation in a wetted wall column. The CO_2 overall mass transfer coefficient(K_G) of DETA/DEA/DMAC exceeded other biphasic solvents, blended amine solution, and 40% K_2CO_3 solution, with 3 times that of 40% K_2CO_3 solution. Moreover, various operational conditions including absorption temperature, gas flow rate, and water content of solution were taken into account to build a multiple-condition kinetic mechanism to offer guidance for biphasic absorbents. Furthermore, phase separation behavior was revealed as the main blame for the deterioration in the liquid film chemical mass transfer process of biphasic solvents in the CO_2 absorption process, resulting in the k_L of DETA/DEA/DMAC before phase separation decreased by 75.3% at the phase separation stage. Therefore, it is crucial to ensure that the CO_2 loading of the solution entering absorber is lower than the phase separation point in applications. After phase separation, DETA/DEA/DMAC split into the organic and aqueous phases, the k_L of the aqueous phase gradually exceeded that of the organic phase as CO_2 loading increased for its higher chemical enhancement factor(E).

1. Introduction

Carbon capture and storage (CCS) technology has shown great potential in greenhouse gas emission reduction for effective decarbonization[1]. Amine solution-based chemical absorption holds great promise in CO_2 capture currently for its advantages such as application flexibility, high CO_2 capture rate, and high safety and stability[2]. However, industry applications of traditional amine absorption, represented by 30 wt% monoethanolamine(MEA) absorbent, have shown problems including high regeneration energy consumption and low cycling capacity, which severely hinder the large-scale industrial operation of chemical absorption[3].

To address this issue, a range of novel amine solvents have been developed for chemical absorption. Among them, biphasic absorbents have garnered significant attention for their lower regeneration energy consumption and higher cyclic capacity[4,5]. Typically, driven by changes in CO_2 loading or temperature, biphasic absorbents gradually separate into two phases including of the aqueous phase and the organic phase in the CO_2 absorption process. Most CO_2 is concentrated in the aqueous phase while the organic phase has very low CO_2 content. Only the aqueous phase is transferred to the stripper for regeneration, which can achieve energy consumption reduction.

Several research has verified that biphasic absorbents can further

* Corresponding authors.
E-mail addresses: oatgnaw@zju.edu.cn (T. Wang), mxfang@zju.edu.cn (M. Fang).

https://doi.org/10.1016/j.cej.2024.154002
Received 23 May 2024; Received in revised form 10 July 2024; Accepted 12 July 2024
Available online 14 July 2024
1385-8947/© 2024 Elsevier B.V. All rights are reserved, including those for text and data mining, AI training, and similar technologies.

Nomenclature

M	The molar concentration (mol/L)	Re	Reynolds number
r	CO_2 absorption rate (mol CO_2/kg·s)	Sc	Schmidt numbers
α	The molality (mol/kg)	R	Ideal gas constant
P_{CO2}*	CO_2 equilibrium vapor pressure (Pa)	d	Hydraulic diameter of the wetted wall column (cm)
H	Henry's Law constant (Pa·cm^3·mol^{-1})	h	Height of the wetted wall column (cm)
N_{CO2}	CO_2 flux (mol/(cm^2•s))	k_L^0	Liquid film physical mass transfer coefficient (cm/s)
q	Molar gas flow rate (mol/s)	u	Liquid flow rate (cm^3/s)
Q	Gas flow rate (L/min)	W	Circumference of the wetted column (cm)
φ	CO_2 volume fraction (%)	A	Gas-liquid contact area of the wetted wall column (cm^2)
V_M	Molar volume of standard gas	ρ	Density (g/cm^3)
K_G	CO_2 overall mass transfer coefficient (mol/(cm^2•s•Pa))	μ	Viscosity (cp)
P_d	Driving force for gas-phase mass transfer (Pa)	g	Gravitational acceleration
k_L	Liquid film mass transfer coefficient (mol/(cm^2•s•Pa))	D	Diffusion coefficient (cm^2/s)
k_g	Gas film mass transfer coefficient (mol/(cm^2•s•Pa))	E	The chemical enhancement factor
Sh	Sherwood number	Ha	The Hatta number
		E_∞	The infinite enhancement factor
		ν	The stoichiometric coefficient

reduce energy consumption while enhancing the cyclic capacity of the solution. Bai et al.[6] developed a non-aqueous N-ethylethanolamine (EMEA)/N,N-diethylethanolamine(DEEA) biphasic solvents which has a low energy consumption of 1.71 GJ/ ton CO_2 and an outstanding cyclic capacity of 3.0 mol/L. Hong et al.[7] proposed 2-(methylamino)ethanol (MAE)/diethylene glycol dimethyl ether(DGM)/water biphasic absorbent with a cyclic capacity of 1.32 mol/L and energy consumption of only 2.28 GJ/ton CO_2. Wang et al.[8] applied 1-propanol as phase separator and diethylenetriamine(DETA) as reactive amine, and then a 30 wt% DETA/50 wt% 1-propanol biphasic absorbent was proposed with a low energy consumption of 2.12 GJ/ ton CO_2. Jin et al[9] developed tetramethylethylenediamine (TMEDA)/MEA/Dimethyl sulfoxide (DMSO) with the highest cyclic capacity of 0.23 mol CO_2/mol amine and low regeneration energy of 2.28 GJ/ ton CO_2.

Apart from regeneration energy and cyclic capacity, the CO_2 mass transfer performance including the CO_2 overall mass transfer coefficient (K_G) as well as liquid film mass transfer coefficient(k_L) is another vital standard in the development of biphasic absorbent. Zhang et al.[4] discovered that most biphasic absorbents with superior absorption mass transfer performance typically exhibit elevated absorption and cyclic capacity. However, it was found that the fluctuation of operational conditions in practical industrial applications is a common issue affecting the efficient absorption mass transfer process of biphasic absorbents[10]. In order to adjust the operational conditions in time and effectively ensure the absorption performance of the absorbent in applications, many studies have been conducted to investigate the factors influencing the K_G of biphasic solution. An et al.[11] investigated the influence of gas flow rate on the overall mass transfer process of DETA/DEEA biphasic absorbent using a wetted wall column(WWC) and the K_G of solution at CO_2 loading of 0.98 mol/L showed a slight increase with rising gas flow rate. Zhang et al.[12] adjusted the absorption temperature to measure the K_G of 1 M(mol amine/L(amine + H_2O)) TETA/3M N, N-dimethylcyclohexylamine (DMCA) biphasic solvent by a WWC and the K_G of solutions at various CO_2 loading rose as temperature increased. However, in the study by Wang et al[13], the K_G of the N,N-dimethylbutylamine (DMBA)/DEEA biphasic absorbent with high CO_2 loading occurred reduction with a rise of temperature. Although various operation conditions were found to be impact factors that would affect the K_G of biphasic solutions, a comprehensive kinetic analysis on the influencing mechanism of different operation parameters to the k_L which represents the CO_2 absorption mass transfer of biphasic solutions, remains absent either. A systemic kinetic mechanism guidance for biphasic absorbents is urgently needed for widespread industrial utilization of biphasic solvents.

Moreover, studies have indicated that the CO_2 absorption would weaken the K_G of the biphasic absorbent[14]. Wang et al.[15] investigated the K_G of triethylenetetramine (TETA)/DEEA biphasic absorbent at various CO_2 loading in a WWC at 318 K and the K_G of solvent at CO_2 loading of 1.23 mol/L was 74.5 % lower than that of unloaded solution. Zhang et al.[12] measured the K_G of TETA/DMCA biphasic solvent at various CO_2 loading in 313 K and the K_G of solution at 0.75 mol CO_2/mol amine was 8.7 % lower than that of solvent at 0.25 mol CO_2/mol amine. Moreover, according to studies about the phase separation mechanism of physical solvent-based biphasic absorbents, amines in biphasic absorbents gradually convert to carbamates in the CO_2 absorption process, which exhibit significantly higher polarity in water compared to organic solvents[16,17]. The polarity difference causes carbamates to preferentially associate with water, while physical solvents gradually precipitate at phase separation stage with increasing CO_2 loading. Upon reaching a critical CO_2 loading, which was referred to as the phase separation point, the single-phase solution eventually completes its separation into biphasic solution including the aqueous and organic phases, showing differences in amine concentration and phase CO_2 loading between each phase after phase separation[17,18]. For instance, the DETA amine concentration in the aqueous phase of saturated DETA/diethanolamine(DEA)/N, N-dimethylacetamide(DMAC) biphasic solution was 1.92 mol CO_2/kg (amine + H_2O) after phase separation, which was 6.6 times that of organic phase[19]. The phase separation behavior of biphasic solvents within absorber could be an essential factor for the absorption mass transfer process of absorbents and the stability of absorber[20,21]. Moreover, it would continue to affect the CO_2 absorption kinetics of both the organic and aqueous phases after phase separation. However, kinetic research on the phase separation behavior of biphasic solvents, is limited at present.

A typical amide-based biphasic absorbent, DETA/DEA/DMAC/H_2O (2DE1AC) solvent was proposed with the viscosity regulation of DEA on the DETA/DMAC/H_2O(DEAC) solvent in our previous study[19], which has great potential in CO_2 capture for its great superiority in the reduction of regeneration energy and the enhancement of cyclic capacity. To reveal the CO_2 absorption kinetics of the absorbent. In this work, DETA/DEA/DMAC was selected as the subject of systemic kinetic investigation in a WWC. A method for determining the phase separation point of physical solvent-based biphasic absorbents by measuring the inflection point of the CO_2 absorption reaction rate curve was proposed. The CO_2 absorption kinetic parameters of absorbents were obtained. A multiple-condition kinetic mechanism for biphasic absorbents considering various operational conditions including absorption temperature, gas flow rate, and water content of solutions was built. The kinetic analysis of 2DE1AC and DEAC biphasic absorbents in the CO_2 absorption process was investigated. The impact of phase separation behavior on the CO_2 absorption kinetics of biphasic solutions was revealed. The CO_2 equilibrium partial pressure and Henry's constants of the biphasic absorbents under various operating conditions were measured in a Vapor-liquid equilibria (VLE) setup.

Finally, this study aims to provide an efficient biphasic absorbent and offer guidance for the design base, as well as the adjustment of operating conditions in the CO_2 chemical absorption process.

2. Experiments

2.1. Material

DMAC(≥99.5 %), DETA(≥99 %), DEA(≥99 %) were all obtained from Aladdin. Pure CO_2, N_2, and N_2O gases were obtained from Hangzhou Jingong GAS Co., Ltd, Hangzhou, China.

2.2. Experimental setup

2.2.1. CO_2 absorption experiment

According to Chen et al[19] and Hu et al[22], for physical solvent-based biphasic absorbents, the CO_2 absorption reaction rates r_{CO2}(mol CO_2/kg(amine + H_2O)·s), which measured the amount of CO_2 absorbed per unit mass of absorbent solution per unit time, as depicted in Eq. S1, would occur significant decrease at specific CO_2 loading which was exactly the phase separation point of biphasic solvent.

Therefore, using a bubbling reactor column(Fig. S1), the instantaneous CO_2 absorption rate r_{CO2} curves of 2DE1AC and DEAC solution were measured at 303, 313, 323, and 333 K(the measurement process was provided in the Supplementary Material). The inflection point of the r_{CO2} in the absorption process for each solution, indicating the phase separation points, was determined. As seen in Fig. S2, the phase separation point of 2DE1AC and DEAC at various temperatures was 1.39 mol CO_2/kg (amine + H_2O) and 1.48 mol/kg, respectively. At this point, two immiscible phases were first observed in the 2DE1AC and DEAC solution during the CO_2 absorption process, as seen in Fig. S3 d) and Fig. S4 d).

Additionally, 2DE1AC and DEAC solutions at various CO_2 loading in the CO_2 absorption process were prepared by weighing method at 313 K (the preparation process was provided in the Supplementary Material). The mass ratio of DETA: DEA: DMAC: H_2O in the 2DE1AC solution was kept at 13 %: 7 %: 40 %: 40 %. The mass ratio of DETA: DMAC: H_2O in the DEAC solution was kept at 20 %: 40 %: 40 %. The states of various solutions after settling were recorded in Figs. S3 and S4. The phase separation points for 2DE1AC and DEAC solution were further validated in the Supplementary Material. The CO_2 loading measured by acid-base titration as well as amine concentration in the aqueous and organic phases of various solutions obtained using Cation Ion Chromatography (IC) at 313 K were listed in Table S1 and Table S2.

$$\alpha_{CO2} = \frac{m_c}{M_{rCO2} \bullet (m_{sol} + m_c/1000)} \quad (1)$$

Where α_{CO2} denotes the CO_2 loading of solution, mol CO_2/kg (amine + H_2O), m_c represents the change in mass of the absorbent before and after CO_2 absorption, g. m_{sol} represents the mass of the solution involved in the absorption reaction, kg. M_{rCO2} is the molecular weight of CO_2, 44 g/mol.

2.2.2. Wetted-wall column

As seen in Fig. 1, the main setup of the WWC(9) consists of two layers. The outer layer was used to regulate the temperature stability of the inner layer using a water bath(10)(at the temperature of 303, 313, 323, and 333 K) and the inner layer was the reaction zone. The WWC has a diameter of 1.2 cm, a height of 8.31 cm, and a gas–liquid contact area of 31.328 cm^2. A mixed gas of CO_2 and N_2, under the control of mass flow controllers(3) (SEC-E40-V, accuracy 0.5 %), passed through a vapor saturator(4) to form saturated gas with water vapor and subsequently entered the bottom of the WWC. The CO_2 partial pressure was controlled

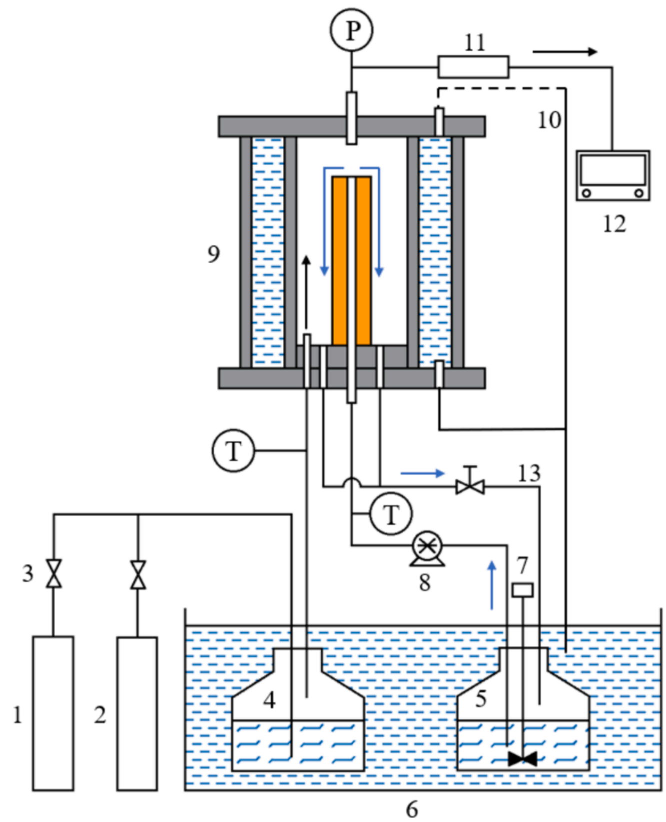

Fig. 1. The WWC setup schematics (1) CO_2 gas, (2) N_2 gas, (3) mass flow controllers, (4) gas saturation bottle, (5) solution tank, (6) water bath, (7) agitator, (8) pump, (9) wetted wall column, (10) constant temperature water bath, (11) drying tube, (12) CO_2 analyzer, (13) reflux pipe.

at 2.03 to 10.13 kPa, while the gas flow rate ranged from 1 to 3 L/min. The prepared absorbents at different CO_2 loading were stored in a tank (5), totaling 1.5 L. A gear pump(8) was used to pump the solutions to the WWC continuously to form a uniform liquid film (flow rate of 200 ml/min). At this point, gas and liquid underwent countercurrent contact in the WWC, where CO_2 absorption reaction and mass transfer occurred. The CO_2 volume fraction in the mixed gas after the reaction was recorded through a CO_2 analyzer(12) (GHX-3010F, accuracy 1 %). The solutions after the reaction returned to the solution tank(5) via the reflux pipe(13) to facilitate recycling experiments. The temperature of the incoming gas and liquid was monitored using two thermocouples.

To simulate the homogeneous state of solutions under flow disturbances in the practical absorber. All solutions were maintained in a homogeneous state under agitation by an overhead stirrer(7) (rotating at 350 r/min) in the experiments. Among them, for the 2DE1AC and DEAC mixed solutions at CO_2 loading of 1.5 and 1.7 mol/kg after phase separation, although it would generate immiscible aqueous and organic phases after settling, it failed to phase splitting under agitation and kept in homogeneous states, as seen in Fig. S3 g) and i) and Fig. S4 g) and i). The homogeneous states of solutions after phase separation in the WWC were verified in the Supplementary Material. The measurement for the CO_2 loading of solution after phase separation was also provided in the Supplementary Material. The CO_2 loading of solutions remained stable during a batch experiment.

However, it was difficult to maintain the homogeneous state of the solution at the phase separation point under stirring disturbance. The solution was found to easily revert from the unstable biphasic state depicted in Fig. S3 (e) and Fig. S4 (e) back to a single-phase state in Fig. S3 (c) and Fig. S4 (c). The instability of the solution state could potentially affect the accuracy of experimental analysis. Therefore, in this study, the phase separation stage of 2DE1AC and DEAC solutions

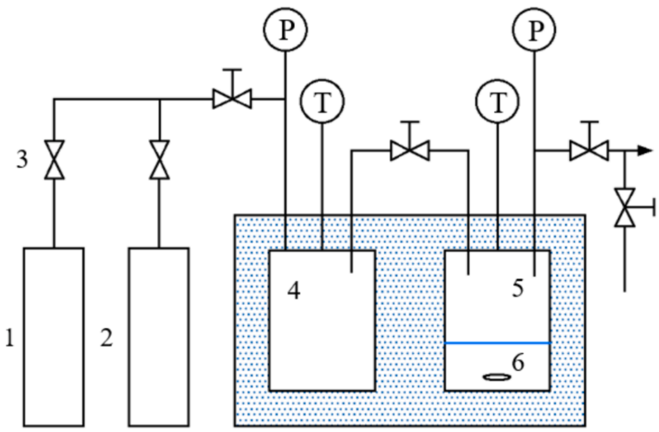

Fig. 2. The Vapor-liquid equilibria (VLE) apparatus schematics (1) N_2O gas, (2) CO_2 gas, (3) mass flow controllers, (4) gas vessel, (5) reactor, (6) magnetic stirring, (7) constant temperature water bath.

was established between 1 to 1.5 mol/kg because this range closely corresponded to the phase separation points of solutions. It can not only effectively reflect the CO_2 absorption mass transfer characteristic at the phase separation stage of solutions, but also demonstrate good experimental stability, which was advantageous for the kinetic analysis on the CO_2 absorption at phase separation stage. Moreover, CO_2 loading from 0 to 1 mol/kg was designated as the before separation stage to ensure that the solution had not yet undergone phase separation. CO_2 loading from 1.5 to 1.7 mol/kg was identified as the after phase separation stage, as shown in Fig. S3 and Fig. S4.

The CO_2 absorption kinetic parameters of the solutions at CO_2 loading of 0, 1, 1.5, and 1.7 mol/kg under various conditions were measured using the WWC. Subsequently, the solution was separated into the organic and aqueous phase using a separatory funnel, and their kinetic parameters were measured separately at 313 K.

2.2.3. Vapor-liquid equilibria

The Vapor-liquid equilibria (VLE) apparatus schematics is shown in Fig. 2. The method corresponds to that applied by Sutar et al.[23], Jagushte and Mahajani[24] and Nath[25].

The volume of reactor(5) V_r and gas vessel(4) V_g is 485 cm^3 and 500 cm^3, respectively. The volume of the absorbent added, V_1, is controlled within the range of 60–100 ml. The speed of magnetic stirring(6) was kept at 200 r/min, where the solutions of the biphasic absorbents remained homogeneous at this speed after phase separation. The temperature inside the reactor and gas vessel was controlled by a constant temperature water bath(7). The equilibrium vapor pressure P_{CO2}* of CO_2 in the solvent and the N_2O Henry's Law constant, H_{N_2O} at various temperature can be obtained by introducing different gas(CO_2 and N_2O) into the VLE device[26].

We measured the CO_2 solubility of 30 wt% MEA using the VLE apparatus in Fig. 2 at 313 K and 373 K, and compared it with literature data[27–30], as shown in Fig. S6. The experiment data are listed in Table S7. As seen in Fig. S6, the CO_2 solubility in this work is in line with the published data, especially in the CO_2 partial pressure range of (3–150) kPa. Thus, the VLE setup and experimental method are reliable.

2.3. Dynamics parameters

2.3.1. Kinetic parameters

The CO_2 flux N_{CO2} (mol/(cm^2•s)) entering the absorbent solution per unit time in the WWC can be calculated using Eq. (2):

$$N_{CO2} = \frac{q_{CO2,in} - q_{CO2,out}}{A} \tag{2}$$

Where A represents the gas–liquid contact area of the WWC. $q_{CO2,in}$ and $q_{CO2,out}$ denote the inlet and outlet CO_2 flow rates of the WWC, respectively, mol/s. These values are calculated according to Eq. (3) and (4).

$$q_{CO2,in} = \frac{Q_{gas}}{60 \bullet V_M} \bullet \frac{T_s}{T_i} \bullet \varphi_{CO2,in} \tag{3}$$

$$q_{CO2,out} = \frac{(100 - \varphi_{CO2,in}) \bullet Q_{gas}}{(100 - \varphi_{CO2,out}) \bullet V_M \bullet 60} \bullet \frac{T_s}{T_i} \bullet \varphi_{CO2,out} \tag{4}$$

$\varphi_{(CO2,in)}$ and $\varphi_{(CO2,out)}$ denote the CO_2 volume fraction of the mixture gas entering and exiting the WWC, respectively, %. Q_{gas} denotes the gas flow rate at the inlet of the WWC, L/min. V_M represents the ideal gas molar volume at standard condition, which is 22.4 L/mol, T_s represents standard condition temperature, 273 K.T_i denotes absorption temperature, K.

The CO_2 overall mass transfer coefficient K_G (mol/(cm^2•s•Pa)) for the WWC can be calculated using Eq. (5).

$$K_G = \frac{N_{CO2}}{P_d} \tag{5}$$

Where P_d is the driving force for gas-phase mass transfer, calculated by Eq. (6).

$$P_d = \frac{(P_{in} - P^*_{CO2}) - (P_{out} - P^*_{CO2})}{In(\frac{P_{in} - P^*_{CO2}}{P_{out} - P^*_{CO2}})} \tag{6}$$

P_{in} and P_{out} represents the inlet and outlet CO_2 partial pressures in the WWC, calculated by Eq. (7).

$$P_{in(out)} = P \bullet \varphi_{CO2,in(out)} \tag{7}$$

P is the total gas pressure, set to 1 atm in the experiment. P^*_{CO2} represents the CO_2 equilibrium partial pressure of each solution under different conditions, obtained from the VLE experiment in Pa (The P^*_{CO2} of the unloaded solution is 0 Pa).

Using the WWC apparatus, CO_2 absorption mass transfer of 30 % MEA was measured to validate the experimental method, as depicted in Fig. 3.

As shown in Fig. 3, the relative error of CO_2 flux under each driving force was within 3 % compared with the data from the literature[30], indicating the correctness of the experimental method.

According to the two-film theory[31], in the WWC, the gas phase and the liquid phase counter-currently contact each other, forming gas and

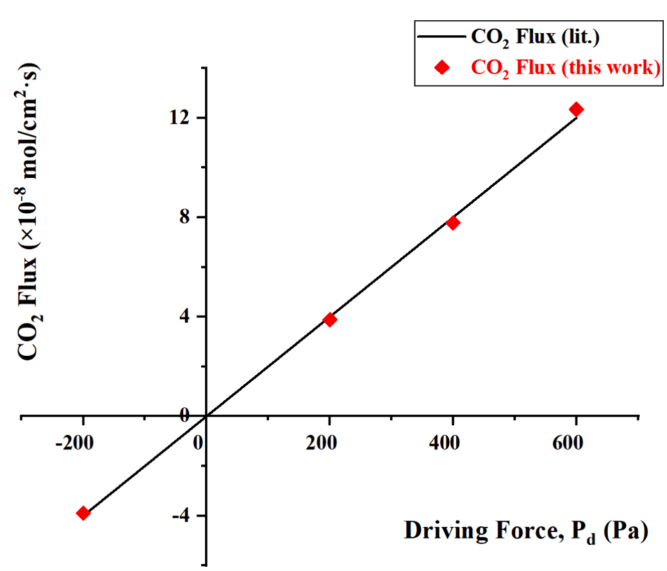

Fig. 3. Validation of CO_2 absorption in 30 % MEA under different driving force measured by the WWC at 313 K.

liquid films on both sides of the gas–liquid contact surface. CO_2 initially diffuses from the gas phase to the gas film. The majority of CO_2 is subsequently rapidly consumed by chemical reaction with the absorbent near the liquid film area, while a small portion of CO_2 and reaction products diffuse from the liquid film and enter the liquid phase. Due to the large Q_{gas} and volume of the solution, the composition of the gas and liquid bulks (i.e., the absorption solution) can be considered constant in the experiment. The K_G is composed of the liquid film mass transfer coefficient k_L (mol/(cm^2•s•Pa)) and the gas film mass transfer coefficient k_g (mol/(cm^2•s•Pa)), as shown in Eq.8.

$$\frac{1}{K_G} = \frac{1}{k_L} + \frac{1}{k_g} \tag{8}$$

The k_g represents the diffusion mass transfer process of CO_2 from the gas phase to the gas film, which is decided by the geometric dimensions of the WWC equipment and the gas flow rate, which can be obtained from Eq. (9) and Eq.10[32].

$$Sh = 1.075\left(Re \cdot Sc \cdot \frac{d}{h}\right)^{0.85} \tag{9}$$

$$Sh = \frac{k_g \cdot R \cdot T \cdot d}{D_{CO2,g}} \tag{10}$$

Sh is Sherwood number. Where d and h are the hydraulic diameter and height of the WWC, cm. R denotes ideal gas constant, 8.314 J/(mol·K). T is the temperature of gas, K. $D_{CO2,g}$ represents the CO_2 diffusion coefficient in the gas phase, cm^2/s. Re and Sc are Reynolds and Schmidt numbers, respectively, as depicted in Supplementary Material.

The k_L represents the absorption mass transfer process of CO_2 through the gas film into the liquid film of the absorbent which comprises chemical reaction and physical diffusion, as depicted in Eq. (11) [33]. The chemical reaction is influenced by the reaction characteristics of the absorbent composition, while physical diffusion is affected by the physical properties of the absorbent, Q_{gas}, as well as the geometric dimensions of the WWC.

$$k_L = \frac{E \cdot k_L^0}{H_{CO2,sol}} \tag{11}$$

Where k_L^0 represents the liquid film physical mass transfer coefficient, cm/s, as depicted in Eq. (12)[31]. E denotes the chemical enhancement factor. $H_{CO2,sol}$ represents the Henry's constant of CO_2 in different absorbents under various conditions, Pa•cm^3/mol, and obtained from VLE experiments.

$$k_L^0 = \left(\frac{3^{\frac{1}{3}} \bullet 2^{\frac{1}{2}}}{\pi^{\frac{1}{2}}}\right) \bullet \left(\frac{u_l^{\frac{1}{3}} \bullet h^{\frac{1}{2}} \bullet W^{\frac{2}{3}}}{A}\right) \bullet \left(\frac{\rho g}{\mu}\right)^{\frac{1}{6}} \bullet D_{CO2,sol}^{\frac{1}{2}} \tag{12}$$

Where u_l represents the solution flow rate. W represents the circumference of the wetted column. ρ denotes the density of solutions, measured by the Kyoto Electronics Manufacturing DA-130 N with a density accuracy of 0.001 g/cm^3. μ denotes the viscosity of solutions, measured by a digital rotational viscometer (DV-II+Pro, accuracy of 1 %). g denotes the gravitational acceleration. $D_{CO2,sol}$ represents the CO_2 diffusion coefficient in the solution.

The chemical enhancement factor E is related to the Hatta number (Ha) and the infinite enhancement factor (E_∞), which can be obtained using Eq. (13) and (14)[34].

$$Ha = \frac{\sqrt{\frac{r_{CO2} D_{CO2,sol}}{\alpha_{CO2}}}}{k_L^0} \tag{13}$$

$$E_\infty = \sqrt{\frac{D_{CO2,sol}}{D_{R,sol}}} \bullet \left(1 + \frac{D_{R,sol}}{D_{CO2,sol}} \bullet \frac{H_{CO2,sol} \bullet \alpha_{R,sol} \bullet \rho_{sol}}{\nu_R \bullet P_d}\right) \tag{14}$$

Where $D_{R,sol}$ is the diffusion coefficient of the absorption reaction product in the solvent, cm^2/s. $\alpha_{R,sol}$ is the concentration of the absorption reaction product in the solvent, respectively, mol/kg. ρ_{sol} is the density of the solvent. ν_R is the stoichiometric coefficient of the absorption reaction product.

When $3 < Ha \ll E_\infty$, the pseudo-first-order reaction can be employed to describe the CO_2 absorption process of absorbents[35]. In this case, E is equal to Ha[36,37]. Eq. (11) can be simplified to:

$$k_L = \frac{\sqrt{\frac{r_{CO2} D_{CO2,sol}}{\alpha_{CO2}}}}{H_{CO2,sol}} \tag{15}$$

2.3.2. Diffusion coefficient

The CO_2 diffusion coefficient in the solvent is dependent on the viscosity of the absorbent and temperature and can be calculated using Eq. (16)[26]. The CO_2 diffusion coefficient in the water at various temperatures can be obtained by Eq. (17).

$$D_{CO2,sol} = D_{CO2,water} \bullet \left(\frac{\mu_w}{\mu}\right)^{0.8} \tag{16}$$

$$D_{CO2,water} = 2.35 \times 10^{-6} \exp(-2119/T) \tag{17}$$

2.4. CO_2 physical solubility

Since the reaction rate between CO_2 and absorbents was rapid, the N_2O analogy method[38] was employed to obtain the Henry's Law constant of CO_2 at different temperatures, which can be obtained using Eq. (18).

$$H_{CO_2,sol} = H_{N_2O,sol}\left(\frac{H_{CO_2,water}}{H_{N_2O,water}}\right) \tag{18}$$

$H_{N_2O,sol}$ can be obtained from VLE experiments. The Henry's Law constants for CO_2 and N_2O in water are as follows[39]:

$$H_{CO_2,water} = 2.82 \times 10^6 \exp(-2044/T) \tag{19}$$

$$H_{N_2O,water} = 8.55 \times 10^6 \exp(-2284/T) \tag{20}$$

3. Results and discussion

3.1. CO_2 overall mass transfer coefficient of 2DE1AC solution

The CO_2 overall mass transfer coefficient(K_G) of the unloaded 2DE1AC solution was measured. Compared the K_G of 2DE1AC solution with two types of lipophilic biphasic absorbents (DMBA/DEEA[13] and DETA/DEEA[11] solutions), traditional 30 wt% MEA[40] solution, MEA/DEEA blended solution[41] and conventional K_2CO_3 solution[42]. As seen in Fig. 4, the K_G of the 2DE1AC solvent was the highest among all biphasic absorbents, being 2–3 times that of other solutions. The K_G of the 2DE1AC solvent was 2.7 times that of the 2 M(mol amine/L(amine + H_2O)) DMBA/4M DEEA solution. Additionally, the K_G of the 2DE1AC solution was 15.0 % and two times higher than that of the 3 M MEA/3M

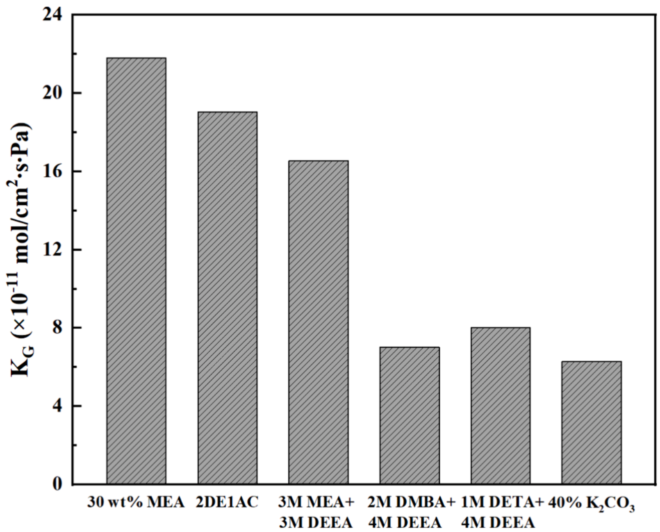

Fig. 4. CO_2 overall mass transfer coefficients of various unloaded solutions at 313 K(gas flow rate at 3 L/min).

DEEA blended amine solution and 40 % K_2CO_3 solution, respectively, indicating that the 2DE1AC solvent has outstanding mass transfer performance in the CO_2 chemical absorption. Limited by the relatively low original amine concentration of the solution, the K_G of the unloaded 2DE1AC solvent was 12.7 % lower than that of the 30 % MEA solution.

3.2. Multiple-condition kinetic mechanism for biphasic absorbent

To provide guidance for adjusting operating parameters and ensuring the efficient CO_2 absorption mass transfer performance of the absorbent, various operational conditions were taken into account to build a multiple-condition kinetic mechanism in this section.

3.2.1. Kinetic mechanism of temperature on absorption mass transfer

To investigate the influence of absorption temperature on the CO_2 absorption mass transfer process of biphasic absorbents, this study selected 303, 313, 323, and 333 K as the absorption temperatures for DEAC and 2DE1AC absorbents under different CO_2 loadings. The liquid film mass transfer coefficient(k_L) of each solution at various CO_2 loading was measured, as shown in Fig. 5. Relevant kinetic parameters are listed in Table 1. The k_g and P_{CO2}* of various solutions under different conditions in this work were listed in the Supplementary Material.

As seen in Fig. 5, it was indicated that for various solutions, the k_L increased gradually with a rise in temperature. For example, when the CO_2 loading was 0 mol/kg, an increase of the temperature from 303 K to 333 K led to a 56.3 % and 75.8 % significant enhancement in k_L for the 2DE1AC and DEAC solutions, respectively.

Analyzed from Table 1, it was found that, for most solutions, the reason for enhanced k_L lay in a rise in both k_L^0 and E with increasing temperature. However, it was noteworthy that for 2DE1AC and DEAC at CO_2 loading of 1 mol/kg, the enhancement effect of rising temperature on E from 323 to 333 K occurred a slight decrease compared with that on E from 303 to 313 K. Specially, rising temperature from 303 to 313 K led to a 5.8 % and 4.2 % improvement in E for 2DE1AC and DEAC solution at CO_2 loading of 1 mol/kg, while rising temperature from 323 to 333 K led to a 4.2 % and 3.1 % enhancement in E for 2DE1AC and DEAC solutions, respectively. Moreover, when the CO_2 loading reached 1.5 mol CO_2/kg(amine + H_2O) and 1.7 mol/kg, increasing temperature even led to a reduction in E for 2DE1AC and DEAC solution, indicating that the CO_2 chemical mass transfer of solutions deteriorated with rising temperature. For instance, the E for the 2DE1AC solution at CO_2 loading of 1.7 mol/kg under 333 K was 25.5 % lower than that of solution under 323 K. For the DEAC mixed solution at CO_2 loading of 1.5 and 1.7 mol/kg, increasing temperature from 303 to 333 K continuously deteriorated the chemical mass transfer process of the solution, resulting in E for DEAC solutions at CO_2 loading of 1.5 and 1.7 mol/kg at 333 K being 21.5 % and 24.4 % lower than that of DEAC at CO_2 loading of 1.5 and 1.7 mol/kg under 303 K, respectively.

Therefore, it was revealed that when the k_L^0 maintained an upward trend with a rise in temperature, the strengthening effect of increasing temperature on the chemical mass transfer gradually weakened, or even reversed with increasing CO_2 loading. It would weaken the improvement effect of rising temperature on the CO_2 absorption mass transfer process of biphasic absorbent, especially in high-loading solutions [11,13]. For example, when the CO_2 loading reached 1.7 mol/kg, the enhancement effect of increasing temperature from 303-333 K only led to a 7.1 % and 13.5 % increase on the k_L for the 2DE1AC and DEAC solutions, respectively, which was significantly weaker than that on k_L for 2DE1AC and DEAC unloaded solutions.

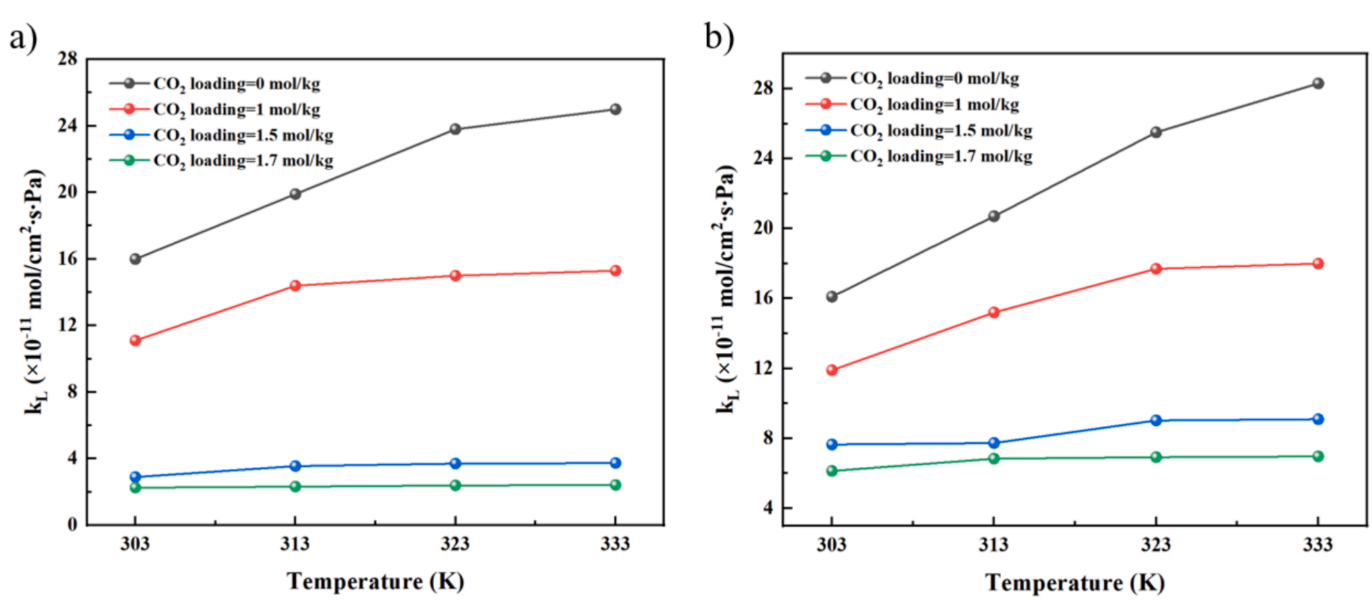

Fig. 5. The liquid film mass transfer coefficient of various solutions under different temperatures (gas flow rate at 3 L/min) (a) 2DE1AC solution (b) DEAC solution.

Table 1
CO_2 absorption kinetic parameters of 2DE1AC and DEAC absorbent. 2DE1AC:

CO_2 [a]	T	Q_{gas}	K_G	k_L	k_L^0	ρ	μ	$D_{CO2,soln}$	$H_{CO2,soln}$	E
(mol/kg)	(K)	(L/min)	($mol\cdot cm^{-2}\cdot s^{-1}\cdot Pa^{-1}$)		(cm/s)	(g/cm^3)	(cp)	(cm^2/s)	($Pa\cdot cm^3\cdot mol^{-1}$)	
0	303	3	1.54E-10	1.60E-10	4.15E-03	1.020	6.47	4.05E-06	1.80E+09	65.6
0	313	3	1.90E-10	1.99E-10	5.22E-03	1.020	4.57	5.71E-06	1.83E+09	70.0
0	323	3	2.25E-10	2.38E-10	6.24E-03	1.020	3.53	7.51E-06	2.67E+09	102.0
0	333	3	2.35E-10	2.50E-10	7.58E-03	1.020	2.98	1.47E-05	3.53E+09	117.4
0	313	1	1.17E-10	1.26E-10	5.22E-03	1.020	4.57	5.71E-06	1.83E+09	44.3
0	313	2	1.71E-10	1.81E-10	5.22E-03	1.020	4.57	5.71E-06	1.83E+09	63.5
0	313	4	1.96E-10	2.04E-10	5.22E-03	1.020	4.57	5.71E-06	1.83E+09	71.5
1	303	3	1.08E-10	1.11E-10	3.30E-03	1.056	9.81	2.91E-06	1.80E+09	59.0
1	313	3	1.39E-10	1.44E-10	4.20E-03	1.056	6.77	4.17E-06	1.83E+09	62.4
1	323	3	1.45E-10	1.50E-10	5.21E-03	1.056	4.91	5.77E-06	2.67E+09	76.8
1	333	3	1.48E-10	1.54E-10	6.80E-03	1.056	3.65	8.90E-06	3.53E+09	80.0
1	313	1	8.78E-11	9.28E-11	4.20E-03	1.056	6.77	4.17E-06	1.83E+09	40.4
1	313	2	1.24E-10	1.29E-10	4.20E-03	1.056	6.77	4.17E-06	1.83E+09	56.2
1	313	4	1.44E-10	1.48E-10	4.20E-03	1.056	6.77	4.17E-06	1.83E+09	64.4
1.5	303	3	2.78E-11	2.80E-11	2.35E-03	1.084	17.97	1.79E-06	1.80E+09	21.3
1.5	313	3	3.53E-11	3.56E-11	2.94E-03	1.084	12.80	2.50E-06	1.83E+09	22.2
1.5	323	3	3.68E-11	3.71E-11	3.67E-03	1.084	9.18	3.50E-06	2.67E+09	27.0
1.5	333	3	3.70E-11	3.74E-11	5.04E-03	1.084	6.25	5.79E-06	3.53E+09	26.2
1.5	313	1	2.53E-11	2.57E-11	2.94E-03	1.084	12.80	2.50E-06	1.83E+09	16.0
1.5	313	2	3.20E-11	3.23E-11	2.94E-03	1.084	12.80	2.50E-06	1.83E+09	22.0
1.5	313	4	3.64E-11	3.67E-11	2.94E-03	1.084	12.80	2.50E-06	1.83E+09	22.9
1.7	303	3	2.25E-11	2.26E-11	2.17E-03	1.089	20.76	1.60E-06	1.80E+09	18.8
1.7	313	3	2.31E-11	2.32E-11	2.85E-03	1.089	13.56	2.39E-06	1.83E+09	14.9
1.7	323	3	2.38E-11	2.39E-11	3.38E-03	1.089	10.62	3.11E-06	2.67E+09	23.6
1.7	333	3	2.41E-11	2.42E-11	4.54E-03	1.089	7.52	4.99E-06	3.53E+09	18.8
1.7	313	1	1.70E-11	1.72E-11	2.85E-03	1.089	13.56	2.39E-06	1.83E+09	11.0
1.7	313	2	1.81E-11	1.82E-11	2.85E-03	1.089	13.56	2.39E-06	1.83E+09	11.7
1.7	313	4	2.33E-11	2.34E-11	2.85E-03	1.089	13.56	2.39E-06	1.83E+09	15.0

DEAC:

CO_2 [a]	T	Q_{gas}	K_G	k_L	k_L^0	ρ	μ	$D_{CO2,soln}$	$H_{CO2,soln}$	E
(mol/kg)	(K)	(L/min)	($mol\cdot cm^{-2}\cdot s^{-1}\cdot Pa^{-1}$)		(cm/s)	(g/cm^3)	(cp)	(cm^2/s)	($Pa\cdot cm^3\cdot mol^{-1}$)	
0	303	3	1.55E-10	1.61E-10	4.12E-03	1.017	6.53	4.02E-06	2.39E+09	93.4
0	313	3	1.97E-10	2.07E-10	5.17E-03	1.017	4.63	5.65E-06	2.54E+09	101.9
0	323	3	2.40E-10	2.55E-10	6.20E-03	1.017	3.57	7.44E-06	2.67E+09	110.0
0	333	3	2.64E-10	2.83E-10	7.59E-03	1.017	2.98	1.05E-05	3.13E+09	116.8
0	313	1	1.32E-10	1.44E-10	5.17E-03	1.017	4.63	5.65E-06	2.54E+09	70.7
0	313	2	1.78E-10	1.89E-10	5.17E-03	1.017	4.63	5.65E-06	2.54E+09	92.7
0	313	4	2.04E-10	2.13E-10	5.17E-03	1.017	4.63	5.65E-06	2.54E+09	104.5
1	303	3	1.16E-10	1.19E-10	3.18E-03	1.054	10.46	2.76E-06	2.39E+09	90.1
1	313	3	1.47E-10	1.52E-10	4.13E-03	1.054	6.97	4.07E-06	2.54E+09	93.8
1	323	3	1.70E-10	1.77E-10	4.62E-03	1.054	6.06	4.87E-06	2.67E+09	102.2
1	333	3	1.72E-10	1.80E-10	5.36E-03	1.054	5.56	6.36E-06	3.13E+09	105.4
1	313	1	1.02E-10	1.09E-10	4.13E-03	1.054	6.97	4.07E-06	2.54E+09	67.2
1	313	2	1.41E-10	1.45E-10	4.13E-03	1.054	6.97	4.07E-06	2.54E+09	90.4
1	313	4	1.50E-10	1.55E-10	4.13E-03	1.054	6.97	4.07E-06	2.54E+09	95.3
1.5	303	3	7.51E-11	7.65E-11	2.46E-03	1.075	16.55	1.91E-06	2.39E+09	74.5
1.5	313	3	7.60E-11	7.74E-11	2.78E-03	1.075	14.07	2.32E-06	2.54E+09	70.6
1.5	323	3	8.83E-11	9.03E-11	3.65E-03	1.075	9.25	3.48E-06	2.67E+09	66.0
1.5	333	3	8.90E-11	9.10E-11	4.65E-03	1.075	7.20	5.17E-06	3.13E+09	61.3
1.5	313	1	5.68E-11	5.89E-11	2.78E-03	1.075	14.07	2.32E-06	2.54E+09	51.7
1.5	313	2	6.95E-11	7.11E-11	2.78E-03	1.075	14.07	2.32E-06	2.54E+09	64.8
1.5	313	4	7.81E-11	7.94E-11	2.78E-03	1.075	14.07	2.32E-06	2.54E+09	72.4
1.7	303	3	6.05E-11	6.14E-11	2.03E-03	1.080	23.14	1.46E-06	2.39E+09	72.3
1.7	313	3	6.73E-11	6.84E-11	2.65E-03	1.080	15.34	2.17E-06	2.54E+09	65.4
1.7	323	3	6.81E-11	6.93E-11	2.99E-03	1.080	13.14	2.62E-06	2.67E+09	61.8
1.7	333	3	6.85E-11	6.97E-11	3.75E-03	1.080	10.50	3.83E-06	3.13E+09	58.1
1.7	313	1	5.15E-11	5.32E-11	2.65E-03	1.080	15.34	2.17E-06	2.54E+09	50.7
1.7	313	2	6.34E-11	6.47E-11	2.65E-03	1.080	15.34	2.17E-06	2.54E+09	61.9
1.7	313	4	6.91E-11	7.01E-11	2.65E-03	1.080	15.34	2.17E-06	2.54E+09	67.0

[a] mol CO_2/kg (amine + water).

3.2.2. *Kinetic mechanism of gas flow rate on absorption mass transfer*

Gas flow rate can be one of the important factors that may influence the k_L of biphasic absorbents. This study selected 1, 2, 3, and 4 L/min as Q_{gas} for DEAC and 2DE1AC absorbents under different CO_2 loadings and the k_L of each solution was measured.

As shown in Fig. 6, Table 1, and Table S3, it can be observed that for both 2DE1AC and DEAC solutions, the k_L kept increasing with a rise of Q_{gas}, which was mainly attributed to the improvement of both E and k_g for each solution. When CO_2 loading was 0 mol/kg, increasing Q_{gas} from 1 to 4 L/min led to a 61.9 % and 47.9 % significant enhancement in k_L for the 2DE1AC and DEAC solutions, respectively. However, as seen in Fig. 6, the enhancement effect of increasing Q_{gas} from 3 to 4 L/min on the k_L of various 2DE1AC and DEAC solutions was limited, leading to the steady k_L between solutions at Q_{gas} of 3 L/min and 4 L/min.

Additionally, analyzed from Table 1, the enhancement effect of rising Q_{gas} on the k_L of 2DE1AC and DEAC solution diminished with increasing CO_2 loading. For instance, at CO_2 loading of 1.5 mol/kg, increasing Q_{gas} from 1 to 4 L/min led to a 42.8 % and a 34.8 % increase

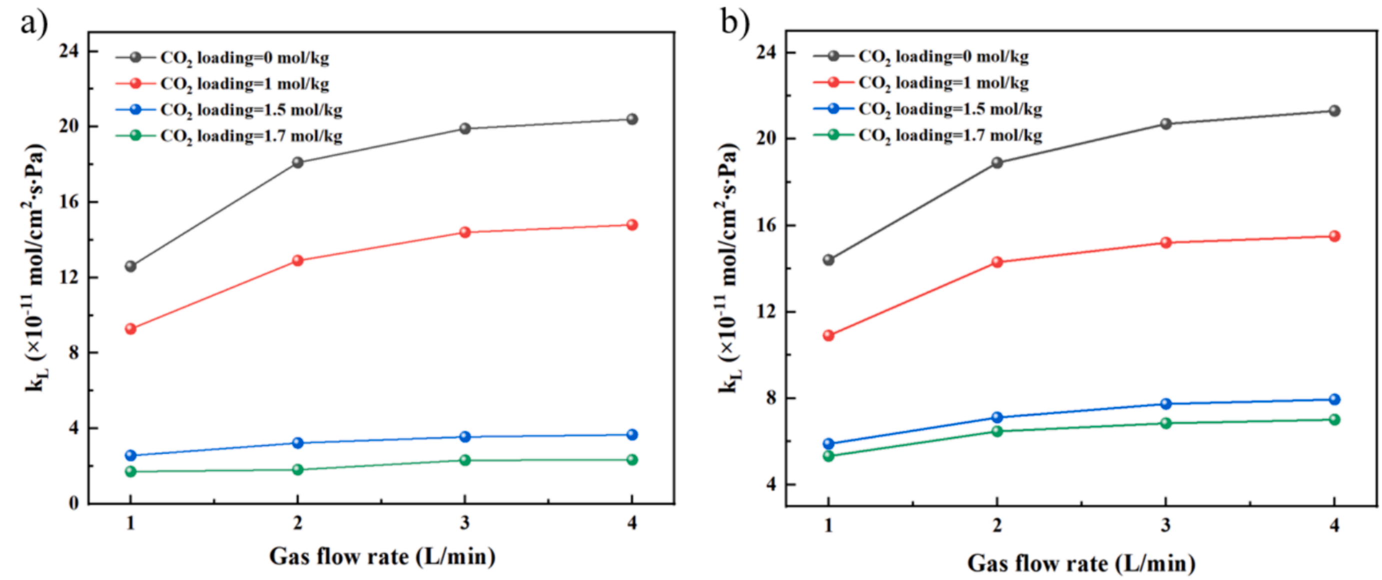

Fig. 6. The liquid film mass transfer coefficient of various solutions under different gas flow rate at 313 K (a) 2DE1AC solution (b) DEAC solution.

in k_L for 2DE1AC and DEAC, which was weaker than that in the k_L for the 2DE1AC and DEAC unloaded solutions. When the CO_2 loading reached 1.7 mol/kg, the enhancement effect of increasing Q_{gas} from 1 to 4 L/min only led to a 36.0 % and 31.8 % increase on the k_L for the 2DE1AC and DEAC solutions, respectively. It was indicated that the reason lay in the fact that the enhancement effect of increasing Q_{gas} on the chemical mass transfer process in the liquid film gradually weakened for high-loading solutions, leading to a deterioration of the rise in E with increasing gas flow rate. In this case, when the CO_2 loading was 0 mol/kg, the E of 2DE1AC and DEAC solutions increased by 61.4 % and 47.8 %, respectively, as the gas flow rate rose from 1 to 4 L/min. However, when the CO_2 loading was 1.7 mol/kg, the enhancement effect of increasing Q_{gas} from 1 to 4 L/min on the E for the 2DE1AC and DEAC solutions decreased to 36.4 % and 32.1 %, respectively. As a result, the sensitivity of the k_L to Q_{gas} gradually decreased with increasing CO_2 loading.

In conclusion, for the adjustment of absorption temperature as well as gas flow rate, biphasic solutions at relatively low CO_2 loading within absorber would be easier to regulate the absorption performance, which is advantageous for the operation efficiency.

3.2.3. Kinetic mechanism of solution water content on absorption mass transfer

To analyze the kinetic impact mechanism of water content on the CO_2 absorption mass transfer of 2DE1AC biphasic absorbents at various CO_2 loading. In this section, the mass ratio of H_2O in the 2DE1AC solution is altered (with initial amine concentrations of DETA and DEA unchanged), resulting in DETA/DEA/DMAC(50 wt%)/H_2O(30 wt%) and DETA/DEA/DMAC(30 wt%)/H_2O(50 wt%) biphasic solvents as well as DETA/DEA aqueous solution. The k_L of each solution at various CO_2 loading was measured, as indicated in Fig. 7. Relevant kinetic parameters are listed in Table 2.

As seen in Fig. 7, when the water content decreased from 40 % to 30 % in the 2DE1AC biphasic solvent, the k_L of the solution showed a slight decrease at various CO_2 loading. Meanwhile, increasing water content from 40 % to 50 % decreased k_L for 2DE1AC at 0 and 1 mol/kg CO_2 loading, while slightly enhancing the k_L in the solution at CO_2 loading reached 1.5 and 1.7 mol/kg. The opposite impact of increasing water mass ratio on the k_L of the 2DE1AC solution at different CO_2 loading persisted until the 2DE1AC transformed into DETA/DEA aqueous solution.

As indicated in Fig. 8, it can be observed that for the DETA/DEA/DMAC biphasic solvents, a rise in water mass ratio resulted in higher k_L^0 values and lower E values at various CO_2 loadings. It can be revealed that for amide-based biphasic absorbents, an increase in water content can enhance the physical mass transfer process, which was associated with a decrease in solution viscosity and an increase in CO_2 diffusion coefficients in the solutions, as seen in Table 2. On the other hand, increasing water content would deteriorate the chemical mass transfer in the liquid film between the absorbent and CO_2 and lead to lower E.

Therefore, when the water content of the solution decreased from 40 % to 30 %, the physical mass transfer process in the 2DE1AC solution at CO_2 loadings of 0 and 1 mol/kg was weakened, leading to a decrease of 15.3 % and 20.5 % in k_L^0 for each solution, respectively. However, the E of 2DE1AC only increased by 4.6 % and 9.8 % in this case compared to DETA/DEA/DMAC (50 wt%)/H_2O (30 wt%) at CO_2 loadings of 0 and 1 mol/kg, respectively. Moreover, when the CO_2 loading reached 1.5 and 1.7 mol/kg, CO_2 absorption led to a decrease in the concentration of active amines in the solution, resulting in relatively low E values [14]. At this moment, a decrease in water content from 40 % to 30 % only led to a 9.9 % and 10.1 % increase in E for the 2DE1AC at CO_2 loading of 1.5 and

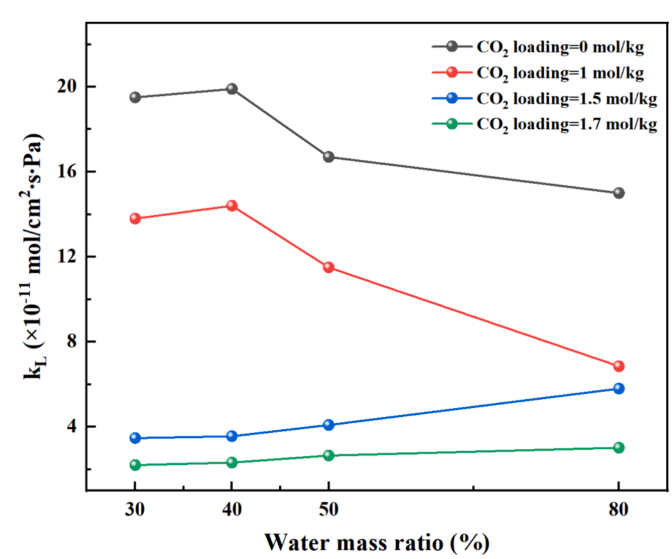

Fig. 7. The liquid film mass transfer coefficients of DETA/DEA/DMAC biphasic solutions with different water mass ratio and DETA/DEA aqueous solution at 313 K(gas flow rate at 3 L/min).

Table 2
CO_2 absorption kinetic parameters of aqueous DEAC and 2DE1AC solution at 313 K[a].

CO_2 (mol/kg)	K_G (mol·cm^{-2}·s^{-1}·Pa^{-1})	k_L	k_L^0 (cm/s)	ρ (g/cm^3)	μ (cp)	$D_{CO2,soln}$ (cm^2/s)	$H_{CO2,soln}$ (Pa·cm^3·mol^{-1})	E
DETA/DEA/DMAC(50 %)/H_2O(30 %)								
0	1.86E-10	1.95E-10	4.42E-03	1.025	5.26	4.52E-06	1.66E+09	73.2
1	1.34E-10	1.38E-10	3.34E-03	1.058	7.12	3.02E-06	1.66E+09	68.5
1.5	3.44E-11	3.47E-11	2.36E-03	1.087	18.78	1.84E-06	1.66E+09	24.4
1.7	2.19E-11	2.20E-11	2.23E-03	1.093	20.96	1.69E-06	1.66E+09	16.4
DETA/DEA/DMAC(30 %)/H_2O(50 %)								
0	1.59E-10	1.65E-10	5.74E-03	1.017	3.85	6.55E-06	2.13E+09	61.0
1	1.08E-10	1.11E-10	4.97E-03	1.053	5.01	5.30E-06	2.13E+09	47.0
1.5	4.05E-11	4.09E-11	4.27E-03	1.076	6.60	4.25E-06	2.13E+09	20.4
1.7	2.63E-11	2.65E-11	3.98E-03	1.087	7.51	3.84E-06	2.13E+09	14.2
DETA/DEA/H_2O								
0	1.45E-10	1.50E-10	8.37E-03	1.014	1.98	1.11E-05	2.51E+09	45.0
1	6.74E-11	6.85E-11	7.73E-03	1.051	2.30	9.89E-06	2.51E+09	22.2
1.5	5.72E-11	5.80E-11	7.63E-03	1.075	2.37	9.65E-06	2.51E+09	19.1
1.7	3.00E-11	3.02E-11	7.59E-03	1.085	2.40	9.56E-06	2.51E+09	12.0

[a] k_g = 4.12E-9 mol·cm^{-2}·s^{-1}·Pa^{-1}.

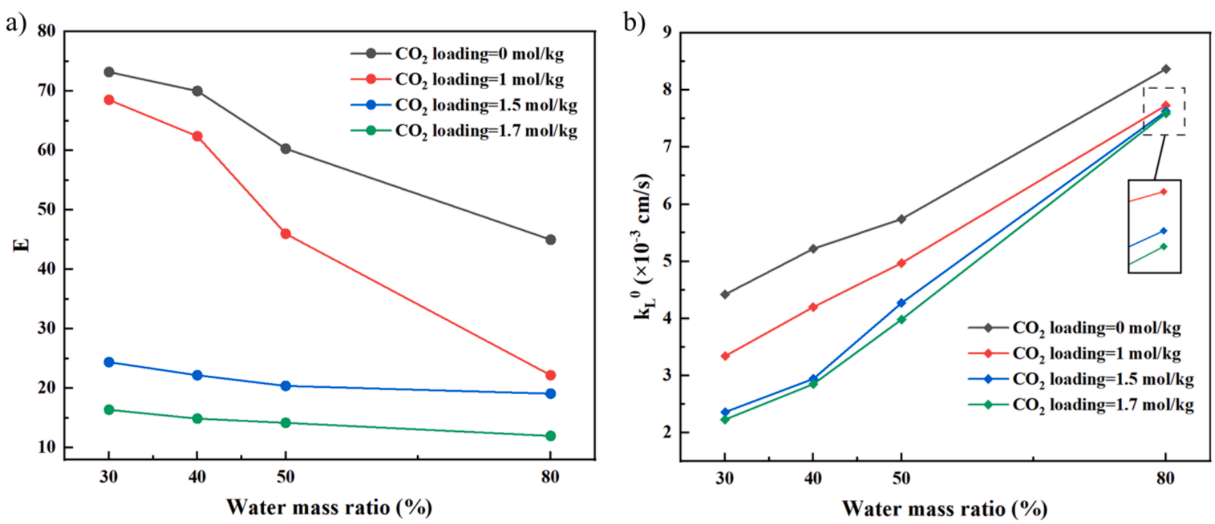

Fig. 8. The liquid film mass transfer process of the DETA/DEA/DMAC biphasic solutions with different water mass ratio and DETA/DEA aqueous solution at 313 K (gas flow rate at 3 L/min) (a) The chemical enhancement factor of various solutions, (b) The liquid film physical mass transfer coefficient of various solutions.

1.7 mol/kg, respectively, while it still notably weakened the physical mass transfer process, resulting in a 19.7 % and 21.8 % decrease in k_L^0 for 2DE1AC solution at CO_2 loading of 1.5 and 1.7 mol/kg, respectively. Therefore, for 2DE1AC solution at various CO_2 loading, the weakening effect of decreasing water content on the CO_2 absorption physical mass transfer process dominated the variation in k_L of the 2DE1AC solution, leading to a slight decrease in k_L for the solution. For instance, at CO_2 loading of 0 and 1 mol/kg, the k_L of DETA/DEA/DMAC(50 wt%)/H_2O (30 wt%) was 2.1 % and 4.3 % lower than that of 2DE1AC at CO_2 loading of 0 and 1 mol/kg, respectively.

As the water content gradually increased in the 2DE1AC solution, the k_L^0 of various 2DE1AC solutions was enhanced, as observed in Fig. 8. Among them, the k_L^0 in the DETA/DEA/DMAC (30 wt%)/H_2O (50 wt%) solution at CO_2 loadings of 0 and 1 mol/kg was 9.9 % and 18.3 % higher than that in the 2DE1AC, respectively. However, rising water content from 40 % to 50 % exhibited great weakening effect on the E of 2DE1AC at CO_2 loadings of 0 and 1 mol/kg, leading to a decrease of 12.9 % and 24.7 % at each 2DE1AC solution, respectively. In this case, the variation in k_L of 2DE1AC at CO_2 loading of 0 and 1 mol/kg was primarily influenced by the weakening impact of rising water content on the CO_2 chemical absorption mass transfer, resulting in a 17.1 % and 22.9 % decrease for the k_L of each solution as water mass ratio increased from 40 % to 50 %. Moreover, the k_L of the DETA/DEA aqueous solution was 32.7 % lower than that of 2DE1AC solution.

Therefore, for the 2DE1AC solution at CO_2 loadings of 0 and 1 mol/kg which commonly encountered in absorber, fluctuation of solution water content in industrial operations, whether decreased or increased, would weaken the CO_2 absorption mass transfer for biphasic solvents. Thus, to avoid the deterioration in the absorption performance of absorbents, measures should be taken to maintain steady water content in the circulation system of the absorbent.

When CO_2 loading reached 1.5 and 1.7 mol/kg, a decrease in the concentration of active amines in the solution led to lower E values. As shown in Fig. 8, at this point, the weakening effect of increasing water content on E gradually diminished. Specifically, a rise in water content from 40 % to 50 % resulted in a decrease of 8.1 % and 4.7 % in E for the 2DE1AC solution at 1.5 and 1.7 mol/kg, respectively. At the same time, the difference of k_L^0 between the 2DE1AC and DETA/DEA/DMAC(30 wt %)/H_2O(50 wt%) further widened. An increase in solution water content from 40 % to 50 % resulted in a significant strengthening effect of 45.2 % and 39.6 % in k_L^0 for the 2DE1AC solution at CO_2 loadings of 1.5 and 1.7 mol/kg, respectively. Therefore, for high-loading 2DE1AC solutions, the primary factor influencing k_L variation shifted to the enhancement impact in CO_2 absorption physical mass transfer with increasing water content. At this stage, the variation trend of k_L for 2DE1AC solutions at CO_2 loading of 0 and 1 mol/kg as water content increased from 40 % to 50 % reversed, showed an increase of 14.9 % and 14.2 % in the 2DE1AC solution at CO_2 loadings of 1.5 and 1.7 mol/kg, respectively. Additionally, the k_L of DETA/DEA aqueous solution was 32.7 % and 62.9 % higher than that of 2DE1AC solution at CO_2 loading of 1.5 and 1.7 mol/kg.

3.3. Kinetic analysis of 2DE1AC and DEAC solution in the CO_2 absorption process

The CO_2 absorption behavior of biphasic solvents varied as CO_2 loading increased. To analyze the kinetic characteristics of biphasic absorbents in the CO_2 absorption process, especially the impact of phase separation behavior on the absorption kinetics of biphasic absorbents and relevant mechanisms, the analysis in this section was divided into two parts: kinetic analysis on the overall CO_2 absorption process and kinetic analysis on the phase separation behavior of biphasic absorbents.

3.3.1. Kinetic analysis on the overall CO_2 absorption process

The liquid film mass transfer coefficient(k_L) of 2DE1AC and DEAC mixed solutions under different CO_2 loading were investigated in Fig. 9.

Overall, the k_L of the absorbent gradually decreased with increasing CO_2 loading. During the transition from 0 to 1.7 mol/kg of CO_2 loading, the k_L of 2DE1AC and DEAC solutions significantly decreased by 88.3 % and 67.0 %, respectively.

Analyzed from Table 1, it was mainly due to the decrease in the k_L^0 and E of the absorbent, which was associated with the rising viscosity, weakening CO_2 diffusion coefficient, and deteriorating reactivity of DETA and DEA amine species in 2DE1AC and DEAC solutions with increasing CO_2 loading. Specially, for 2DE1AC solution, the k_L^0 and E decreased by 45.4 % and 78.7 % in the CO_2 absorption process from 0 to 1.7 mol/kg, respectively. For DEAC solution, the k_L^0 and E decreased by 48.7 % and 35.8 % in the CO_2 absorption process from 0 to 1.7 mol/kg, respectively.

Moreover, for the DEAC and 2DE1AC systems, DETA, as a tertiary amine with three amino groups, had a stronger CO_2 absorption capacity than DEA. Consequently, under the same CO_2 loading, DEAC solutions exhibited higher E values than 2DE1AC solutions, while k_L^0 values were relatively close, which resulted in lower k_L values for 2DE1AC solutions compared to DEAC solutions.

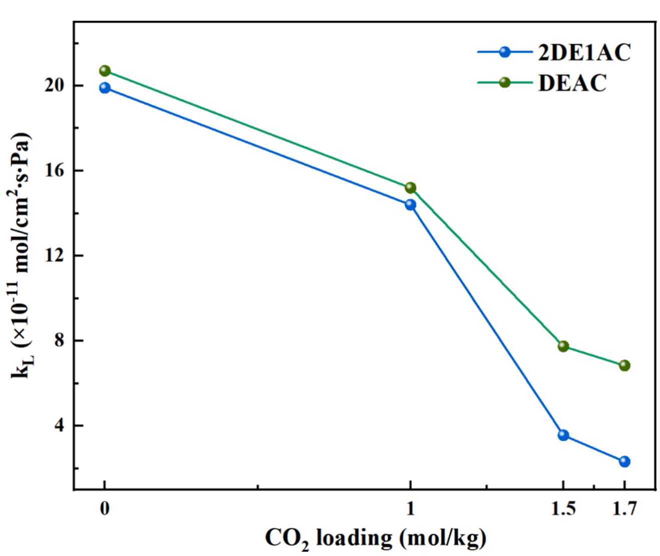

Fig. 9. The liquid film mass transfer coefficients of 2DE1AC and DEAC solution at different CO_2 loading at 313 K (gas flow rate at 3 L/min).

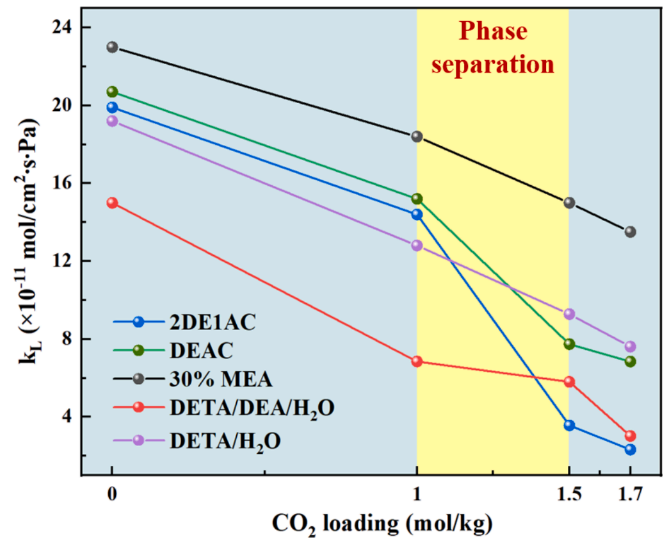

Fig. 10. The liquid film mass transfer coefficients of various solutions in different CO_2 loading at 313 K (gas flow rate at 3 L/min).

3.3.2. Kinetic analysis on the phase separation behavior of biphasic absorbents

As seen in Fig. 9, it was found that the k_L of 2DE1AC and DEAC decreased sharply at the CO_2 loading of 1 to 1.5 mol/kg, which was exactly the phase separation stage of 2DE1AC and DEAC in the CO_2 absorption process. To reveal the CO_2 absorption kinetic characteristics of biphasic absorbents, the k_L of various types of solutions including single amine solution, blended amine solution, and biphasic solvents, were obtained in Fig. 10.

As seen in Fig. 10, for unloaded solutions, the k_L of 2DE1AC and DEAC was higher than that of DETA/H_2O and DETA/DEA blended amine solutions. With a rise in CO_2 loading, CO_2 absorption gradually weakened the k_L of various absorbents. However, as indicated in Fig. 10, the slope of the k_L-CO_2 loading curves of 2DE1AC and DEAC biphasic absorbents at the phase separation stage was much higher than that of 30 wt% MEA, DETA and DETA/DEA aqueous solution. It was revealed that the weakening effect of CO_2 absorption on the k_L of biphasic absorbents at phase separation stage was significantly stronger than that on the single amine as well as blended amine solutions whose the rate of decrease in k_L remained relatively stable as CO_2 loading increased. It led to greater deterioration in k_L of 2DE1AC and DEAC biphasic solvents, resulting in the k_L of 2DE1AC and DEAC being surpassed by DETA/DEA and DETA aqueous solutions, respectively. After phase separation, the rate at which k_L decreased with increasing CO_2 loading gradually slowed down compared to that at the phase separation stage for both 2DE1AC and DEAC.

Therefore, phase separation behavior was assumed to be the main blame for the deterioration of the k_L for biphasic absorbents in the whole CO_2 absorption process. Specially, analyzed from Table 1, it was indicated that the k_L of 2DE1AC mixed solution at CO_2 loading of 1 mol/kg significantly decreased by 75.3 % at phase separation stage, while it reduced by 27.6 % and 34.8 % at before and after phase separation stage, respectively. Likewise, for DEAC solutions, the k_L of absorbent at CO_2 loading of 1 mol/kg decreased by 49.1 % at phase separation stage, while it reduced by 26.6 % and 11.6 % at before and after phase separation stage.

Analyzed from Table 1, it was indicated that the main reason for this phenomenon was the weakening effect of CO_2 loading variation on the both liquid film physical and chemical mass transfer of the solution significantly enhanced during phase separation. For the 2DE1AC solution, before phase separation, a rise in CO_2 loading from 0 to 1 mol/kg led to a decrease of 19.5 % and 10.9 % in k_L^0 and E of solution, respectively, whereas during the phase separation stage, the decreases in k_L^0

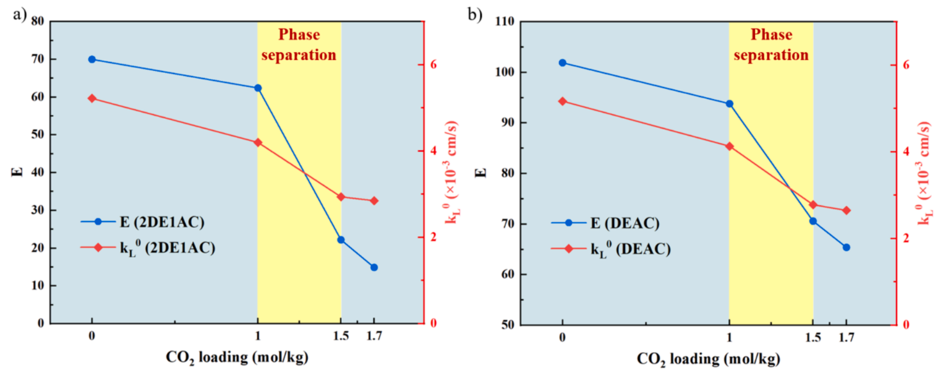

Fig. 11. The liquid film mass transfer process of the 2DE1AC and DEAC biphasic solutions in the CO_2 absorption process at 313 K(gas flow rate at 3 L/min) (a) 2DE1AC solution (b)DEAC solution.

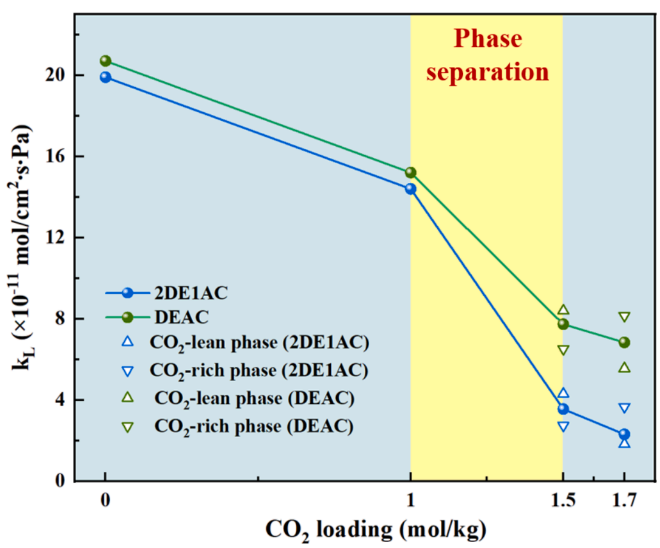

Fig. 12. The liquid film mass transfer coefficients of the CO_2-lean, CO_2-rich, and mixed solution in various CO_2 loading at 313 K(gas flow rate at 3 L/min).

and E of 2DE1AC with a rise in CO_2 loading from 1 to 1.5 mol/kg jumped to 30.0 % and 64.4 %, respectively. Similarly, for the DEAC solution, before phase separation, the decrease in k_L^0 and E was 20.1 % and 7.9 %, respectively, whereas during the phase separation stage, these decreases increased to 32.7 % and 24.7 %, respectively. For biphasic absorbents, the phase separation behavior primarily involves the transfer and accumulation of amine species in the CO_2-rich phase, as seen in Tables S1 and S2. This process would significantly weaken the CO_2 absorption mass transfer in the liquid film, particularly the liquid film chemical mass transfer, thereby reducing the k_L, as seen in Fig. 11.

In order to guarantee an efficient absorption mass transfer performance of biphasic solvents and system stability, it is crucial to ensure that the CO_2 loading of the solution entering absorber is lower than the phase separation point in industrial operation.

Additionally, to investigate the impact of phase separation behavior on the CO_2 absorption kinetics of the organic and aqueous phases after phase separation, the k_L of the CO_2-lean and CO_2-rich phase was measured separately after phase separation as shown in Fig. 12 and the kinetic parameters were listed in Table 3.

By comparing the value of k_L in the CO_2-rich, and CO_2-lean phase at different CO_2 loadings after phase separation, it was observed that the relative magnitudes of k_L between the CO_2-rich phase and the CO_2-lean phase varied in the CO_2 absorption process. After phase separation, as shown in Fig. 12, it was revealed that when CO_2 loading reached 1.5 mol/kg, the k_L of each solution exhibited the order of CO_2-lean phase > CO_2-rich phase; whereas at a CO_2 loading of 1.7 mol/kg, this order changed to CO_2-rich phase > CO_2-lean phase.

As seen in Tables 3, S1, S2, and Fig. 13, it was indicated that at a CO_2 loading of 1.5 mol/kg which was close to the phase separation points of 2DE1AC and DEAC, the transfer and accumulation of amine species in the aqueous phase was limited. It resulted in the amine concentration, phase CO_2 loading as well as chemical enhancement factor in the organic phase being relatively close to those in the aqueous phase. Specifically, for the 2DE1AC solution, the total amine concentration (including DETA and DEA species) and the phase CO_2 loading of the aqueous phase was 40.9 % and 12.5 % higher than that of the organic phase, respectively. And the E in the aqueous phase was 1.8 times that in the organic phase. For the DEAC solution, the total amine concentration (including DETA and DEA species) and the phase CO_2 loading of the aqueous phase was 56.1 % and 19.0 % higher than that of the organic phase, respectively. And the E in the aqueous phase was 1.2 times that in the organic phase. However, due to the higher diffusion coefficient of CO_2 in the organic physical solvent which was associated with relatively low viscosity of the organic phase, the k_L^0 in the organic phase of the 2DE1AC solution was 2.1 times that in the aqueous phase, and for the DEAC solution, the k_L^0 in the organic phase was 1.7 times that in the aqueous phase. Therefore, at this point, the comparison of k_L between the organic and aqueous phases was mainly influenced by the liquid film physical mass transfer, resulting in the k_L of the organic phase exceeding that of the aqueous phase.

As the CO_2 loading reached 1.7 mol/kg, most amine species transited and accumulated in the aqueous phase. Specially, the total amine concentration(including DETA and DEA species) in the aqueous phase of the 2DE1AC and DEAC solution was 2.8 and 3.5 times significantly higher than that of each organic phase, respectively. And the phase CO_2 loading of the aqueous phase for 2DE1AC and DEAC was 8.3 and 13.6 times that of the organic phase in each solution, respectively. Consequently, there was a significant increase in E in the aqueous phase. Among them, the E in the aqueous phase of the 2DE1AC and DEAC solution was 9.1 and 4.8 times that in each organic phase, respectively. In this case, the k_L^0 of the aqueous phase of 2DE1AC and DEAC solutions was 3.0 and 2.8 times

Table 3
CO_2 absorption kinetic parameters of the CO_2-lean, CO_2-rich and mixed solution of 2DE1AC and DEAC after phase separation at 313 K[a].

CO_2 (mol/kg)	Solution state	K_G (mol·cm^{-2}·s^{-1}·Pa^{-1})	k_L	k_L^0 (cm/s)	ρ (g/cm^3)	μ (cp)	$D_{CO2,soln}$ (cm^2/s)	$H_{CO2,soln}$ (Pa·cm^3·mol^{-1})	E
2DE1AC									
1.5	Homogeneous	3.53E-11	3.56E-11	2.94E-03	1.084	12.80	2.50E-06	1.83E+09	22.2
1.5	CO_2-lean	4.27E-11	4.31E-11	4.66E-03	1.046	5.61	4.84E-06	1.79E+09	16.6
1.5	CO_2-rich	2.73E-11	2.75E-11	2.23E-03	1.139	21.16	1.67E-06	2.43E+09	30.0
1.7	Homogeneous	2.31E-11	2.32E-11	2.85E-03	1.089	13.56	2.39E-06	1.83E+09	14.9
1.7	CO_2-lean	1.87E-11	1.88E-11	5.43E-03	1.036	4.27	6.03E-06	1.71E+09	5.9
1.7	CO_2-rich	3.65E-11	3.68E-11	1.79E-03	1.171	31.59	1.22E-06	2.61E+09	53.8
DEAC									
1.5	Homogeneous	7.60E-11	7.74E-11	3.27E-03	1.075	14.07	2.32E-06	2.54E+09	70.6
1.5	CO_2-lean	8.23E-11	8.40E-11	3.83E-03	1.048	7.94	3.67E-06	2.84E+09	62.3
1.5	CO_2-rich	6.43E-11	6.53E-11	2.24E-03	1.102	20.8	1.82E-06	2.50E+09	72.9
1.7	Homogeneous	6.73E-11	6.84E-11	2.65E-03	1.080	15.34	2.17E-06	2.54E+09	65.4
1.7	CO_2-lean	5.49E-11	5.56E-11	5.03E-03	1.021	4.87	5.42E-06	2.37E+09	26.2
1.7	CO_2-rich	8.00E-11	8.16E-11	1.82E-03	1.143	30.21	1.26E-06	2.80E+09	124.3

[a] k_g = 4.12E-9 mol·cm^{-2}·s^{-1}·Pa^{-1}.

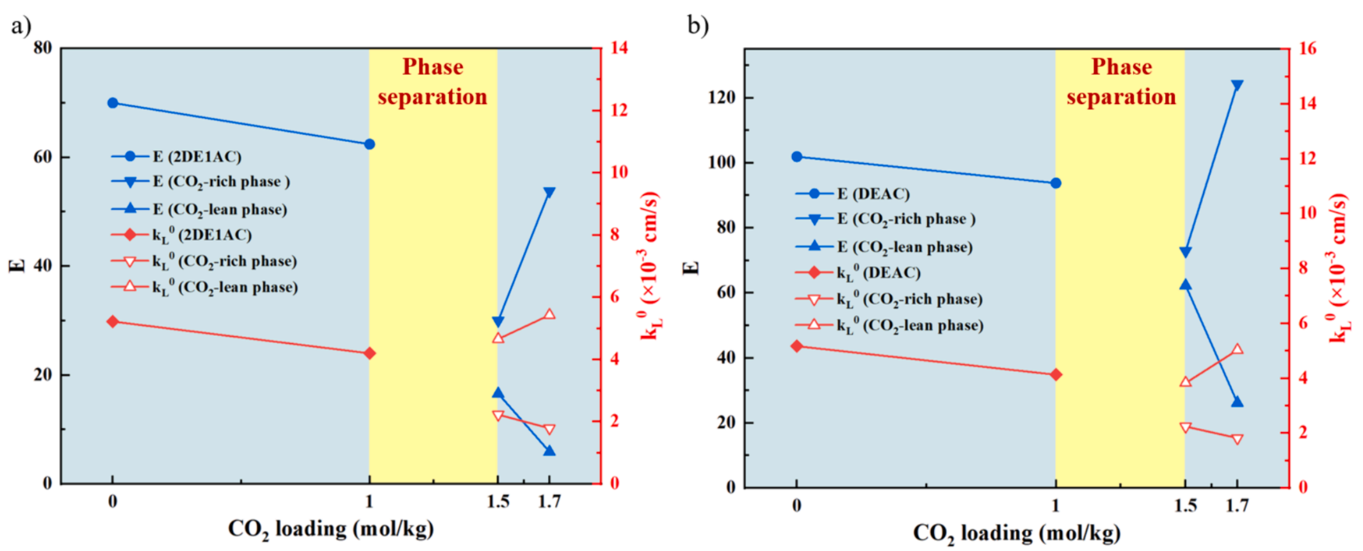

Fig. 13. The liquid mass transfer process of the mixed, CO_2-rich, and CO_2-lean phase of 2DE1AC and DEAC biphasic solutions at various CO_2 loading at 313 K(gas flow rate at 3 L/min) (a)2DE1AC solution (b)DEAC solution.

that of their organic phase, respectively. Therefore, the chemical mass transfer process dominated the comparison of k_L at this point, resulting in the k_L of the aqueous phase exceeding that of the organic phase as well as the mixed solution.

4. Conclusion

The overall mass transfer coefficient (K_G) of DETA/DEA/DMAC exceeded other biphasic solvents, blended amine solution as well as 40 % K_2CO_3 solution, with 3 times that of 40 % K_2CO_3 solution. Increasing absorption temperature and gas flow rate has significant enhancement effect on the liquid film mass transfer coefficient(k_L) of DETA/DEA/DMAC, while it would weaken with increasing CO_2 loading. A rise in water content would enhance the liquid film physical mass transfer process while weakening the chemical mass transfer between the absorbent and CO_2 for amide-based biphasic absorbents.

Phase separation behavior was revealed as the main blame for the deterioration in the liquid film chemical mass transfer of biphasic solvents in the CO_2 absorption process, resulting in the k_L of DETA/DEA/DMAC before phase separation decreased by 75.3 % at the phase separation stage. Therefore, solution at CO_2 loading being lower than phase separation point within absorber is advantageous for the operation efficiency. After phase separation, DETA/DEA/DMAC split into the organic and aqueous phases, it was found that the k_L in the aqueous phase of biphasic solutions gradually exceeded that of the organic phase with increasing CO_2 loading because of its higher chemical enhanced factor(E) which was 9.1 times that of the organic phase.

CRediT authorship contribution statement

Zhipeng Chen: Writing – original draft, Software, Methodology, Investigation, Formal analysis, Conceptualization. **Tao Wang:** Writing – review & editing, Supervision, Resources. **Chao li:** . **Mengxiang Fang:** Writing – review & editing, Supervision, Resources. **Wei Chen:** Funding acquisition. **Ximing Hu:** Funding acquisition. **Yan Shao:** Funding acquisition. **Zhihao Liu:** Funding acquisition. **Wei Zhang:** Funding acquisition. **li Zhang:** Supervision, Methodology. **Wenyang Fan:** Funding acquisition. **Shaojuan Zeng:** Funding acquisition.

Declaration of competing interest

The authors declare that they have no known competing financial interests or personal relationships that could have appeared to influence the work reported in this paper.

Data availability

I would like to submit my data/code if necessary.

Acknowledgment

This work is supported by National Key R&D Program of China (2022YFB4101700, 2023YFE0199300), Pioneer R&D Program of Zhejiang Province -China (2022C03040) , China City Environment Protection Engineering Limited Company cooperation project, and the Fundamental Research Funds for the Central Universities (2022ZFJH004)

Appendix A. Supplementary data

Supplementary data to this article can be found online at https://doi.org/10.1016/j.cej.2024.154002.

References:

[1] Y. Tan, W. Nookuea, H. Li, E. Thorin, J. Yan, Property impacts on Carbon Capture and Storage (CCS) processes: a review, Energy Convers. Manage. 118 (2016) 204–222, https://doi.org/10.1016/j.enconman.2016.03.079.
[2] G.T. Rochelle, Amine scrubbing for CO_2 capture, Science 325 (2009) 1652–1654. https://www.sciencemag.org/lookup/doi/10.1126/science:1176731.
[3] K. Li, W. Leigh, P. Feron, H. Yu, M. Tade, Systematic study of aqueous monoethanolamine (MEA)-based CO_2 capture process: techno-economic assessment of the MEA process and its improvements, Appl. Energy 165 (2016) 648–659, https://doi.org/10.1016/j.apenergy.2015.12.109.
[4] S. Zhang, Y. Shen, L. Wang, J. Chen, Y. Lu, Phase change solvents for post-combustion CO_2 capture: Principle, advances, and challenges, Appl. Energy 239 (2019) 876–897, https://doi.org/10.1016/j.apenergy.2019.01.242.
[5] F. Liu, M. Fang, N. Yi, T. Wang, Research on alkanolamine-based physical-chemical solutions as biphasic solvents for CO_2 capture, Energy Fuel 33 (2019) 11389–11398, https://doi.org/10.1021/acs.energyfuels.9b02392.
[6] L. Bai, S. Lu, Q. Zhao, L. Chen, Y. Jiang, C. Jia, S. Chen, Low-energy-consuming CO_2 capture by liquid-liquid biphasic absorbents of EMEA/DEEA/PX, Chem. Eng. J. 450 (2022) 138490–138500, https://doi.org/10.1016/j.cej.2022.138490.
[7] S. Hong, T. Li, M. Xiao, T. Sema, H. Gao, Z. Liang, A low energy-consuming phase change absorbent of MAE/DGM/H_2O for CO_2 capture, Chem. Eng. J. 480 (2024) 148079–148087, https://doi.org/10.1016/j.cej.2023.148079.
[8] R. Wang, Y. Yang, M. Wang, J. Lin, S. Zhang, S. An, L. Wang, Energy efficient diethylenetriamine-1-propanol biphasic solvent for CO_2 capture: Experimental and theoretical study, Appl. Energy 290 (2021) 116768–116777, https://doi.org/10.1016/j.apenergy.2021.116768.
[9] L. Jin, X. Hou, L. Zhan, S. Xie, L. Gu, H. Yang, X. Wang, X. Qian, J. Shen, L. Yang, Capturing CO_2 using novel nonaqueous biphasic solvent TMEDA/MEA/DMSO: Absorption and phase splitting mechanism, Chem. Eng. J. 484 (2024) 149293–149306, https://doi.org/10.1016/j.cej.2024.149293.
[10] J. Ye, C. Jiang, H. Chen, Y. Shen, S. Zhang, L. Wang, J. Chen, Novel biphasic solvent with tunable phase separation for CO_2 capture: role of water content in mechanism, kinetics, and energy penalty, Environ. Sci. Tech. 53 (2019) 4470–4479, https://doi.org/10.1021/acs.est.9b00040.
[11] S. An, S. Yu, S. Zhang, Y. Zhang, M. Li, Q. Li, L. Wang, Mass transfer characteristics of CO_2 absorption into a phase-change solvent in a wetted-wall column, Int. J. Greenhouse Gas Control 64 (2017) 276–283, https://doi.org/10.1016/j.ijggc.2017.08.001.
[12] S. Zhang, Y. Shen, P. Shao, J. Chen, L. Wang, Kinetics, thermodynamics, and mechanism of a novel biphasic solvent for CO_2 capture from flue gas, Environ. Sci. Tech. 52 (2018) 3660–3668, https://doi.org/10.1021/acs.est.7b05936.
[13] L. Wang, S. An, Q. Li, S. Yu, S. Wu, Phase change behavior and kinetics of CO_2 absorption into DMBA/DEEA solution in a wetted-wall column, Chem. Eng. J. 314 (2017) 681–687, https://doi.org/10.1016/j.cej.2016.12.033.
[14] F. Liu, G.T. Rochelle, T. Wang, E. Chen, M. Fang, CO_2 absorption rate in biphasic solvent of aminoethylethanolamine and diethylethanolamine, Chem. Eng. J. 404 (2021) 126503–126511, https://doi.org/10.1016/j.cej.2020.126503.
[15] L. Wang, S. Liu, R. Wang, Q. Li, S. Zhang, Regulating phase separation behavior of a DEEA-TETA biphasic solvent using sulfolane for energy-saving CO_2 capture, Environ. Sci. Tech. 53 (2019) 12873–12881, https://doi.org/10.1021/acs.est.9b02787.
[16] J. Liu, J. Qian, Y. He, Water-lean triethylenetetramine/N, N-diethylethanolamine/n-propanol biphasic solvents: Phase-separation performance and mechanism for CO_2 capture, Sep. Purif. Technol. 289 (2022) 120740–120752, https://doi.org/10.1016/j.seppur.2022.120740.
[17] L. Yang, J. Chen, N. Ma, Z. Fang, X. Li, Z. Huang, Novel diamine DMAPA-sulfolane-water biphasic absorbent for equimolar CO_2 absorption: Performance and mechanisms, Chem. Eng. J. 479 (2024) 147903–147918, https://doi.org/10.1016/j.cej.2023.147903.
[18] T. Morrison, The salting-out of non-electrolytes. Part I. The effect of ionic size, ionic charge, and temperature, J. Chem. Soc. (resumed) (1952) 3814–3818, https://doi.org/10.1039/JR9520003814.
[19] Z.P. Chen, C. Li, M. Fang, W. Zhang, L. Zhang, W. Fan, H. Hu, Research of novel polyamine-based biphasic absorbents for CO_2 capture using alkanolamine to regulate the viscosity and mechanism analysis, Sep. Purif. Technol. 333 (2024) 125869–125880, https://doi.org/10.1016/j.seppur.2023.125869.
[20] R. Wang, H. Zhao, C. Qi, X. Yang, S. Zhang, M. Li, L. Wang, Novel tertiary amine-based biphasic solvent for energy-efficient CO_2 capture with low corrosivity, Energy 260 (2022) 125045–125055, https://doi.org/10.1016/j.energy.2022.125045.
[21] S. An, X. Huang, N. Li, Q. Li, R. Wang, T. Qi, L. Wang, Comprehensive performance of a diethylenetriamine/2-diethylaminoethanol biphasic absorbent for CO_2 capture, Fuel 353 (2023) 129178–129189, https://doi.org/10.1016/j.fuel.2023.129178.
[22] H. Hu, M. Fang, F. Liu, T. Wang, Z. Xia, W. Zhang, Novel alkanolamine-based biphasic solvent for CO_2 capture with low energy consumption and phase change mechanism analysis, Appl. Energy 324 (2022) 119570–119578, https://doi.org/10.1016/j.apenergy.2022.119570.
[23] P.N. Sutar, P.D. Vaidya, E.Y. Kenig, Activated DEEA solutions for CO_2 capture-A study of equilibrium and kinetic characteristics, Chem. Eng. Sci. 100 (2013) 234–241, https://doi.org/10.1016/j.ces.2012.11.038.
[24] M.V. Jagushte, V.V. Mahajani, Low pressure equilibrium between H_2S and alkanolamine revisited, Indian, J Chem. Technol. 6 (1999) 125–133.
[25] D. Nath, A. Henni, Solubility of carbon dioxide (CO_2) in aqueous solution of 3-(dimethylamino)-1-propylamine (DMAPA), Fluid Phase Equilib. 511 (2020) 112506–112519, https://doi.org/10.1016/j.fluid.2020.112506.
[26] G.F. Versteeg, W. Swaal, Solubility and diffusivity of acid gases (CO_2, N_2O) in aqueous alkanolamine solutions, J. Chem. Eng. Data 33 (1988) 29–34, https://doi.org/10.1021/je00051a011.
[27] K.P. Shen, M.H. Li, Solubility of carbon dioxide in aqueous mixtures of monoethanolamine with methyldiethanolamine, J. Chem. Eng. Data 37 (1992) 96–100, https://doi.org/10.1021/je00005a025.
[28] J.I. Lee, F.D. Otto, A.E. Mather, Equilibrium between carbon dioxide and aqueous monoethanolamine solutions, J. Appl. Chem. Biotechnol. 26 (1976) 541–549, https://doi.org/10.1002/jctb.5020260177.
[29] H. Guo, H. Li, S. Shen, Monoethanolamine+2-methoxyethanol mixtures for CO_2 capture: Density, viscosity and CO_2 solubility, J. Chem. Thermodyn. 132 (2019) 155–163, https://doi.org/10.1016/j.jct.2018.12.028.
[30] U.E. Aronu, S. Gondal, E.T. Hessen, T.H. Warberg, A. Hartono, K.A. Hoff, H. F. Svendsen, Solubility of CO_2 in 15, 30, 45 and 60 mass% MEA from 40 to 120 ℃ and model representation using the extended UNIQUAC framework, Chem. Eng. Sci. 66 (2011) 6393–6406, https://doi.org/10.1016/j.ces.2011.08.042.
[31] R.E. Dugas, Carbon dioxide absorption, desorption, and diffusion in aqueous piperazine and Monoethanolamine, The University of Texas at Austin, 2009.
[32] S. Bishnoi, G.T. Rochelle, Absorption of carbon dioxide into aqueous piperazine: reaction kinetics, mass transfer and solubility, Chem. Eng. Sci. 55 (2000) 5531–5543, https://doi.org/10.1016/S0009-2509(00)00182-2.
[33] H. Yu, Q. Xiang, M. Fang, Q. Yang, P. Feron, Promoted CO_2 absorption in aqueous ammonia, Greenhouse Gases-Science and Technology 2 (2012) 200–208, https://doi.org/10.1002/ghg.1280.
[34] S. Shen, Y. Yang, Y. Bian, Y. Zhao, Kinetics of CO_2 absorption into aqueous basic amino acid salt: potassium salt of lysine solution, Environ. Sci. Tech. 50 (2016) 2054–2063, https://doi.org/10.1021/acs.est.5b04515.
[35] B. Lv, X. Zhou, Z. Zhou, G. Jing, Kinetics and thermodynamics of CO_2 absorption into a novel DETA-AMP-PMDETA biphasic solvent, ACS Sustain. Chem. Eng. 7 (2019) 13400–13410, https://doi.org/10.1021/acssuschemeng.9b02700.
[36] S. Ma, H. Song, M. Wang, J. Yang, B. Zang, Research on mechanism of ammonia escaping and control in the process of CO_2 capture using ammonia solution, Chem. Eng. Res. Des. 91 (2013) 1327–1334, https://doi.org/10.1016/j.cherd.2013.01.020.
[37] K. Li, H. Yu, M. Tade, P. Feron, Theoretical and experimental study of NH_3 suppression by addition of Me(II) ions (Ni, Cu and Zn) in an ammonia-based CO_2

capture process, Int. J. Greenhouse Gas Control 24 (2014) 54–63, https://doi.org/10.1016/j.ijggc.2014.02.019.

[38] I. Amdur, J.W. Irvine, E.A. Mason, J. Ross, Diffusion coefficients of the systems CO_2-CO_2 and CO_2-N_2O, J. Chem. Phys. 20 (1952) 436–443, https://doi.org/10.1063/1.1700438.

[39] A. Clarke, Kinetics of absorption of carbon dioxide in monoethanolamine solutions at short contact times, Ind. Eng. Chem. Fundam. 3 (1964) 239–245, https://doi.org/10.1021/i160011a012.

[40] X. Luo, A. Hartono, H.F. Svendsen, Comparative kinetics of carbon dioxide absorption in unloaded aqueous Monoethanolamine solutions using wetted wall and string of discs columns, Chem. Eng. Sci. 82 (2012) 31–43, https://doi.org/10.1016/j.ces.2012.07.001.

[41] W. Conway, S. Bruggink, Y. Beyad, W. Luo, I.M. Cabrerab, G. Puxtya, P. Feron, CO_2 absorption into aqueous amine blended solutions containing monoethanolamine (MEA), N, N-dimethylethanolamine (DMEA), N, N-diethylethanolamine (DEEA) and 2-amino-2-methyl-1-propanol (AMP) for post-combustion capture processes, Chem. Eng. Sci. 126 (2015) 446–454, https://doi.org/10.1016/j.ces.2014.12.053.

[42] S. Zhang, Y. Lu, Kinetic performance of CO_2 absorption into a potassium carbonate solution promoted with the enzyme carbonic anhydrase: comparison with a Monoethanolamine solution, Chem. Eng. J. 279 (2015) 335–343, https://doi.org/10.1016/j.cej.2015.05.034.